SPANDIDOS PUBLICATIONS

ONCOLOGY REPORTS 49: 39, 2023

DANCR promotes glioma cell autophagy and proliferation via the miR-33b/DLX6/ATG7 axis

WEI YU[1-3], LI MA[1-3] and XINXING LI[1-3]

[1]Department of Neurosurgery, Shengjing Hospital of China Medical University; [2]Liaoning Clinical Medical Research in Nervous Disease; [3]Key Laboratory of Neuro-Oncology in Liaoning, Shenyang, Liaoning 110004, P.R. China

Received August 13, 2022; Accepted December 14, 2022

DOI: 10.3892/or.2023.8476

Abstract. Long non-coding RNAs (lncRNAs) are common in the human body. Misregulated lncRNA expression can cause a variety of diseases in the human body. The present study aimed to investigate the effect of lncRNA differentiation antagonizing non-protein-coding RNA (DANCR) on glioma proliferation and autophagy through the microRNA (miR)-33b/distal-less homeobox 6 (DLX6)/autophagy-related 7 (ATG7) axis. Reverse transcription-quantitative PCR was used to detect DANCR and miR-33b expression. Cell Counting Kit-8 assay and flow cytometry were used to detect cell proliferation and apoptosis, respectively. Transmission electron microscopy was used to determine the autophagy level by observing intracellular autophagosomes. A western blot assay was used to detect protein expression levels and determine the level of autophagy in different cells. The binding sites of miR-33b and DANCR or DLX6 were detected using a dual-luciferase reporter assay. A chromatin immunoprecipitation assay confirmed DLX6 as a transcript of ATG7. *In vivo* tumorigenesis of glioma cells was validated in nude mice. DANCR and DLX6 were highly expressed in glioma cells, while miR-33b showed low expression in glioma cells. DANCR reduced the targeted binding of miR-33b to DLX6 by sponging miR-33b. The result verified that DANCR could promote ATG7 protein expression through miR-33b/DLX6, promote intracellular autophagy and proliferation and reduce apoptosis. The present study identified the role of the DANCR/miR-33b/DLX6/ATG7 axis in regulating autophagy, proliferation, and apoptosis in glioma cells, providing new ideas for glioma treatment.

Correspondence to: Professor Xinxing Li, Department of Neurosurgery, Shengjing Hospital of China Medical University, 36 Sanhao Street, Heping, Shenyang, Liaoning 110004, P.R. China
E-mail: lixx996303@163.com

Abbreviations: lncRNA, long non-coding RNA; DANCR, differentiation antagonizing non-protein coding RNA; HA, human astrocyte; DLX6, distal-less homeobox 6; ATG7, autophagy-related 7; UTR, untranslated region; RT-qPCR, reverse transcription-quantitative PCR; WB, western blot analysis; ChIP, chromatin immunoprecipitation; PVDF, polyvinylidene difluoride; TSS, transcription start site; ceRNA, competing endogenous RNA

Key words: DANCR, microRNA-33b, DLX6, ATG7, autophagy

Introduction

Glioma is the most common adult central nervous system tumor and a primary brain tumor disease (1). Generally, gliomas are diagnosed and classified according to histopathology as astrocytoma, oligodendroglioma, oligodendroastrocytoma and ependymoma. According to the World Health Organization, glioma is generally divided into four grades, among which grade IV glioblastoma has the highest malignancy degree and the worst prognosis. Although patient survival time has been prolonged with the improvement of medical treatment, the five-year survival rate remains consistently low (2,3).

The human genome is widely transcribed, with only ~2% accounting for protein products. Most transcripts do not encode proteins, and RNAs with lengths >200 nucleotides (nt) are named long non-coding RNAs (lncRNAs) (4). Differentiation antagonizing non-protein-coding RNA (DANCR) is an lncRNA associated with the occurrence and progress of various tumors (5). DANCR can promote pancreatic cancer cell proliferation and stemness (6). The proliferation and colony formation of lung cancer cells were positively correlated with the DANCR expression level (7). However, DANCR-mediated autophagy has not been reported in gliomas.

MicroRNA (miRNA) is a class of small non-coding RNA of ~21-22 nt, which can recognize sites in the 3'-untranslated region (UTR) of mRNA and adjust its stability. Furthermore, miRNA usually affects gene expression by targeting mRNA (8,9). Previous studies have shown that abnormal expression of a variety of miRNAs *in vivo* is associated with hidradenitis suppurativa, bladder and gliomas (10-12). Reduced expression of miR-33b is also related to the occurrence of renal cell carcinoma, prostate cancer and medulloblastoma (13-15). However, the relationship between miR-33b and DANCR expression in gliomas has not been reported.

Distal-less homeobox 6 (DLX6) is a homologous transcription factor of DLX5 and the *DLX6* gene is expressed primarily in the brain and skeleton (16). Moreover, DLX6 is involved in the cortical neuron differentiation of precursor cells (17). In their latest study, Liang *et al* (18) found that DLX6 plays a role in the progression of oral squamous cell carcinoma malignancy promoting cell proliferation and survival. Nevertheless, the

function of DLX6 in glioma and its association with posture in glioma cells have not been reported.

Autophagy is a molecular mechanism that maintains the dynamic balance of intracellular ecology, and it can act as a damage repair mechanism when intracellular organelles are damaged. A recent study showed that autophagy-related 7 (ATG7) protects the integrity of human neurons and that its loss leads to degeneration (19). In numerous cases, autophagy is a tumor-promoting factor, and tumor cells require higher levels of autophagy (20,21). ATG7 is an autophagy-associated protein that affects numerous cancer types. Zhu *et al* (22) demonstrated that ATG7 can stabilize the ARHGDIB mRNA by regulating autophagy, thus promoting bladder cancer progression. In 2016, Li *et al* (23) also proposed that ATG7-induced autophagy enhancement is a glioma cell resistance response to the killing effect of temozolomide.

In the present study, the DANCR, miR-33b and DLX6 expression levels were detected in HA, U251 and U87MG cells and the relationship between them was explored. The involvement of the DANCR/miR-33b/DLX6/ATG7 axis in regulating glioma cell autophagy was also explained. The results of the present study may provide novel treatment ideas for glioma.

Materials and methods

Cell culture. The human glioma U87MG (established by J. Ponten and identified by STR profiling) (cat. no. TcHu138), U251 (cat. no. TcHu58) and 293T (cat. no. GNHu17) were purchased from the Chinese Academy of Science (Shanghai, China). The human astrocyte (HA) cells (cat. no. 1800) were purchased from ScienCell Research Laboratories. These cells were cultured in Dulbecco's Modified Eagle Medium (DMEM) (Corning, Inc.) medium containing 10% fetal bovine serum (Procell Life Science & Technology Co., Ltd.) in a humidified incubator at 37˚C with 5% CO_2, and the medium was replaced every 2-3 days or during cell passage until when the cell confluence reached 70-90%.

RNA extraction and reverse transcription-quantitative PCR (RT-qPCR). In the present study, whole-cell RNA was extracted using TRIzol® reagent (Beijing Solarbio Science & Technology Co., Ltd.), RNA concentration was detected using a Nanodrop Spectrophotometer (Thermo Fisher Scientific, Inc.) at a wavelength of 260 nm, and intracellular RNA expression levels were measured using RT-qPCR. DANCR and GAPDH expression was analyzed using HiScript III RT Supermix for qPCR and ChamQ Universal SYBR qPCR Master mix (Vazyme Biotech Co., Ltd.) according to the manufacturer's instructions, Briefly, initial denaturation at 95˚C for 30 sec was followed by 40 cycles of 95˚C for 10 sec and 60˚C for 30 sec. MiRNA-33b and U6 expression was quantified using miRNA 1st Strand cDNA Synthesis kit (stem-loop) and miRNA Universal SYBR qPCR Master mix (Vazyme Biotech Co., Ltd.) according to the manufacturer's instructions. MiRNA-33b primers were designed by software provided by the manufacturer of the miRNA reverse transcription kit, and the universal reverse primer in the kit was used. All RT-qPCR reactions were performed using the 7500 fast RT-PCR System (Thermo Fisher Scientific, Inc.). Finally, each expression was calculated through the $2^{-\Delta\Delta Cq}$ method (24). The primers used in the present study are listed in Table SI.

Cell transfection. Before transfection, $5x10^5$ cells were seeded into 24-well plates, and 1 μg plasmid vector and Lipofectamine 3000 reagent (Thermo Fisher Scientific, Inc.) were mixed according to the manufacturer's instructions and added to the 24-well plates containing cells. After 24 h, the culture medium was replaced, and G418 (500 μg/ml) or puromycin (2 μg/ml) was added to screen the cells containing the plasmid vector, according to the transfection reagent instructions. A full-length DANCR plasmid was constructed with pcDNA 3.1. DANCR [small hairpin (sh-DANCR)] and DLX6 (sh-DLX6) silencing plasmids were constructed with pGPU6. MiR-33b overexpression (pre-mir-33b) and miR-33b interference (anti-miR-33b) plasmids were prepared by Shanghai GenePharma Co., Ltd. All plasmids and negative controls were purchased from Shanghai GenePharma Co., Ltd. The sequences used by the plasmids in the present study are shown in Table SII.

Cell proliferation assay. Cell proliferation assays were performed using the Cell Counting Kit-8 (CCK-8) assay (APeXBIO Technology LLC) in accordance with the manufacturer's instructions. U87MG or U251 cells were seeded in 96-well plates and $3.0x10^3$ cells were added to each well. To determine the OD value, the medium was replaced with 0.1 ml of fresh medium containing 0.01 ml of CCK-8 solution 3 h prior to detection at 24, 48 and 72 h. All of the aforementioned samples were placed in an incubator that contained 5% CO_2 and maintained at 37˚C. Then, the absorbance value at 450 nm was detected with microplate reader (BioTek Instruments, Inc.).

Dual-luciferase reporter assay. Wild-type DANCR (DANCR-wt) and DLX6 (DLX6-wt) sequences containing miR-33b binding sites or mutant DANCR (DANCR-mut) and DLX6 (DLX6-mut) sequences without miR-33b binding sites were inserted into the vector. 293T cells were co-transfected with DANCR-wt + pre-miR-33b, DANCR-wt + pre-NC, DANCR-mut + pre-miR-33b, DANCR-NC + pre-NC, DLX6-wt + pre-miR-33b, DLX6-wt + pre-NC, DLX6-mut + pre-miR-33b, or DLX6-NC + pre-NC in 96-well plates using Lipofectamine 3000 reagent (Thermo Fisher Scientific, Inc.). After 48 h, the dual-Luciferase activity was detected using the Dual-Luciferase® Reporter Assay System (Promega Corporation) according to the manufacturer's instructions. The *Renilla* luciferase activity was used as internal control.

Western blotting (WB). RIPA buffer (Beyotime Institute of Biotechnology) supplemented with 1% protease inhibitor (added 2 min before use) was added to the cells and placed on ice for 30 min. Nucleic acids were crushed with an ultrasonic crusher and centrifuged at 13,800 x g at 4˚C for 30 min. After detection of protein concentration using the bicinchoninic acid (BCA) assay, the loading buffer (5X) was added to the supernatant and heated at 100˚C for 5 min. Proteins were separated using 12 and 10% SDS-PAGE and transferred to 0.22-μm polyvinylidene difluoride (PVDF) membranes (MilliporeSigma). The PVDF membranes were blocked by placing them in Tris-buffered saline containing 0.1% Tween 20 and 5% non-fat

milk at room temperature for 120 min. The membranes were incubated with primary antibodies including DLX6 (1:2,000; cat. no. 23216-1-AP), LC3 (1:5,000; cat no. 14600-1-AP; both from ProteinTech Group, Inc.), p62 (1:1,000; cat. no. 23214; Cell Signaling Technology, Inc.), beclin-1 (1:8,000; cat. no. 66665-1-Ig), ATG7 (1:10,000; cat. no. 67341-1-Ig) and GAPDH (1:20,000; cat. no. 10494-1-AP; all from ProteinTech Group, Inc.) at 4˚C for 14 h. The PVDF membrane was incubated with HRP-conjugated Affinipure Goat Anti-Mouse IgG (H+L) (1:10,000; cat. no. SA00001-1; ProteinTech Group, Inc.) or HRP-conjugated Affinipure Goat Anti-Rabbit IgG (H+L) (1:10,000; cat. no. SA00001-2; ProteinTech Group, Inc.) at room temperature for 2 h. The immunoblot bands were detected using an enhanced chemiluminescence detection kit (ECL kit; Beyotime Institute of Biotechnology), and images were captured using a chemiluminescence imaging analysis system (Bio-Rad Laboratories, Inc.). Finally, the ImageJ 1.53K software (National Institutes of Health) was used to calculate the relative gray value.

Flow cytometry. The required cells were collected according to the manufacturer's instructions (Dojindo Laboratories, Inc.). Briefly, 100 μl of 1X Annexin V binding buffer containing 5 μl of Annexin V-FITC and 5 μl PI was added to the cells, and incubation followed at room temperature for 15 min. Then, 400 μl of 1X Annexin V binding buffer was added to terminate the reaction and the assay was performed on Beckman DxFLEX (Beckman Coulter, Inc.). CytExpert1.1 software (Beckman Coulter, Inc.) was used for analysis. $FITC^{+/}PI^{-}$ cells indicated early apoptosis, and $FITC^{+/}PI^{+}$ cells indicated late apoptosis.

Transmission electron microscopy. Cells were treated with trypsin and centrifuged into clumps, followed by electron microscope fixative (Wuhan Servicebio Technology Co., Ltd.) at room temperature for 30 min, then at 4˚C overnight. Next, they were pre-embedded with agarose, post-fixed, and dehydrated at room temperature. This was followed by resin penetration and embedding using EMBed 812, polymerization, ultrathin sectioning and staining. Briefly, 2% uranium acetate saturated alcohol solution (avoiding light) was used for staining at room temperature for 8 min, then 2.6% Lead citrate (avoiding CO_2) was used for staining at room temperature for 8 min; subsequently, they were put into the grids board and dried overnight at room temperature. Finally, observation and image capturing via transmission electron microscopy was performed (Hitachi, Ltd.).

Chromatin immunoprecipitation (ChIP) assay. A ChIP assay was performed using a Simple Chip Enzymatic Chromatin IP kit (Cell Signaling Technology, Inc.), according to the manufacturer's instructions. Briefly, 1% formaldehyde was added to the cells at room temperature for 10 min to cross-link the protein to the DNA, which was then worked with an ultrasonic crusher (VCX-130, Sonics & Materials, Inc.) at 25% power for 15 sec and repeated 10 times to truncated into fragments of ~600 bp in length. The samples were incubated with anti-DLX6 rabbit antibodies (1:25; cat. no. sc-517058; Santa Cruz Biotechnology, Inc.) or normal rabbit IgG antibodies (1:250; cat. no. 30000-0-AP; ProteinTech Group, Inc.). After DNA cross-links were reversed, and the desired DNA fragment was purified, 2X Tap Master Mix for PAGE (Vazyme Biotech Co., Ltd.) was used to amplify the DNA fragment. The primers used for PCR were as follows: PCR1 forward, 5'-TTCAGCAAGCCACCTAAC-3', and reverse, 5'-AACAAC AAGAGCGATGACT-3'; and PCR2 forward, 5'-TGACAG AGCGAGACTCCGT-3' and reverse, 5'-GGCTGGTCTTGA ACTACTGGA-3'. Finally, agarose electrophoresis was used to verify the PCR products using 3% agarose gels and using SYBR Green staining.

Tumor xenografts in nude mice. First, glioma cells (U87MG) stably expressing sh-DANCR, pre-miR-33b, sh-DLX6 and sh-DANCR + pre-miR-33b + sh-DLX6 were established (n=6). BALB/c nude mice (female; 5 weeks-old; weight, 14-16 g) (Hua FuKang, Beijing, China) were used. Mice were housed under SPF conditions (The temperature of the SPF animal house was between 24-26˚C, the humidity was ~70%, the air exchange rate was 15 times/h, and the light/dark cycle was 12/12 h) and the adequacy of food and water was checked daily to ensure that the mice had access to food and water *ad libitum* at all times. Each mouse was injected with 100 μl PBS containing $1x10^6$ cells subcutaneously under the right armpit. Tumor volumes were recorded on day 7 after injection and then measured every three days. At day 28, the mice were sacrificed by cervical dislocation after inhalation of 3% isoflurane anesthesia and death of mice was confirmed by respiratory arrest. Tumor weights were also compared. The present experiment was approved (approval no. 2022PS021K) by the Medical Ethics Committee of Shengjing Hospital (Shenyang, China).

Immunohistochemistry. After the tumor was removed and fixed with 4% paraformaldehyde at 4˚C for 24 h, it was embedded in paraffin and cut into 5-μm thin sections. After dewaxing with xylene, rehydration (absolute ethanol, 95% ethanol, 90% ethanol, 80% ethanol and 70% ethanol were used for 10 min each in turn), antigen repair, incubation with anti-ATG7 antibodies (1:200; cat. no. 67341-1-Ig; ProteinTech Group, Inc.) at 4˚C overnight, and incubation with biotin-labeled sheep anti-mouse/rabbit IgG polymer (cat. no. KIT-9710; Maxim Biotech, Inc.) at room temperature for 30 min, the tumor was finally stained with diaminobenzidine (Maxim Biotech, Inc.) for 5 min and images were captured under a light microscope (Nikon Corporation).

Bioinformatic analysis. GEPIA (http://gepia.cancer-pku.cn/) was used to analyze the difference in DANCR levels between glioma and normal tissues with a P-value Cutoff of 0.01. The starbase website (https://starbase.sysu.edu.cn) was used to predict potential sites of connection between DANCR and miR-33b. The potential binding sites of DLX6 to the promoter binding region of ATG7 were predicted by JASPAR (https://jaspar.genereg.net).

Statistical analysis. All experiments were repeated at least three times. GraphPad Prism 8 software (GraphPad Software, Inc.) was used for all experimental data, and the results were presented as the mean ± SD. Unpaired student's t-test was used to conduct the comparison between two groups. More than two groups of data were analyzed through a one-way analysis

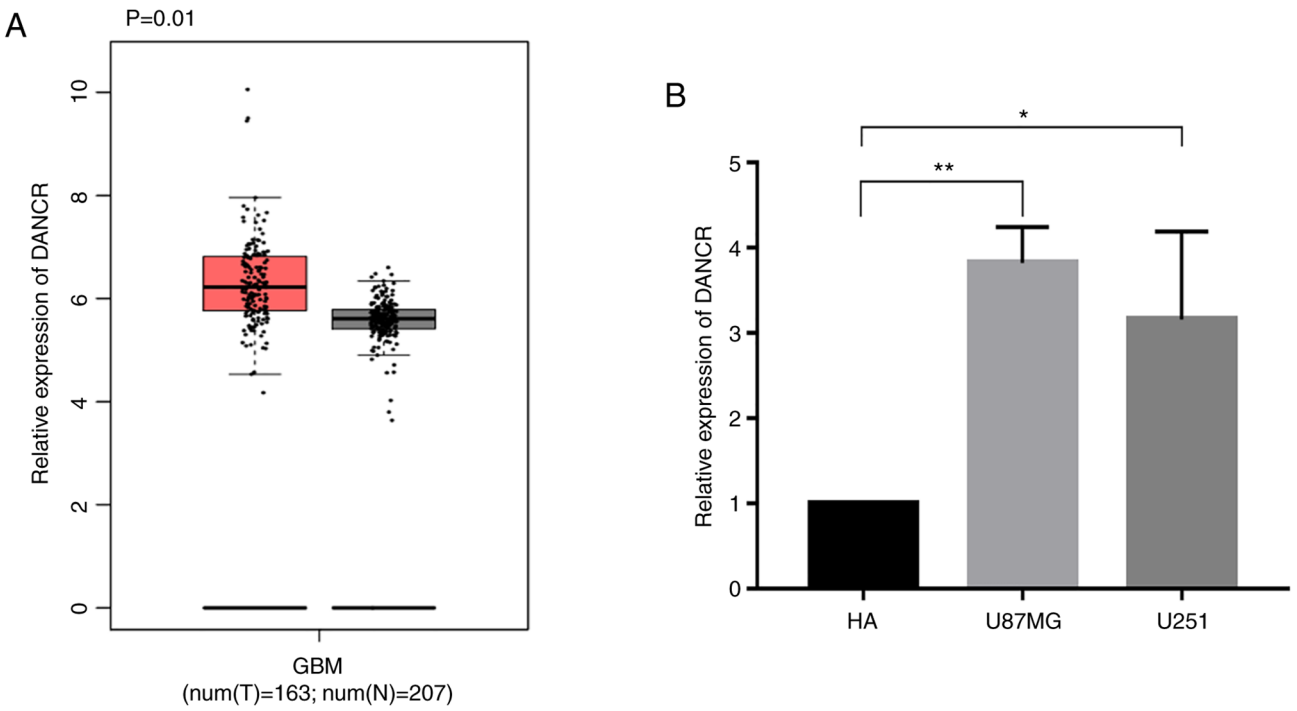

Figure 1. DANCR is highly expressed in glioma cells. (A) GEPIA bioinformatics software was used to analyze DANCR expression in glioma and normal tissues (P=0.01). (B) The relative DANCR expression in the glioma cell lines U87 and U251 was compared with that in normal glial cell line HA using reverse transcription-quantitative PCR (n=3). Data are presented as the mean ± SD. *P<0.05 and **P<0.01. DANCR, differentiation antagonizing non-protein coding RNA; HA, human astrocytes.

of variance followed by LSD post hoc test. P<0.05 was considered to indicate a statistically significant difference.

Results

DANCR is upregulated in glioma. To identify the relationship between DANCR and gliomas, GEPIA (gepia.cancer-pku.cn) was used to preliminarily verify the DANCR expression level in glioma. A higher expression of DANCR was identified in glioma tissues compared with normal tissue (Fig. 1A). Then, the relative expression of DANCR was detected in HA, U251 and U87MG cells using RT-qPCR. It was revealed that the DANCR expression level was higher in the glioma cell lines U251 and U87MG than in HA cells (Fig. 1B).

DANCR regulates autophagy, proliferation and apoptosis in glioma cells. To study the function of DANCR in glioma cells, DANCR-overexpressing U251 and U87MG cell lines were constructed via transfection of the pcDNA3.1-DANCR plasmid vectors into U251 and U87MG cells. Meanwhile, DANCR-silenced U251 and U87MG cell lines were constructed via transfection of the sh-DANCR plasmid vectors in U251 and U87MG cells. First, DANCR expression levels were in DANCR-overexpressing or DANCR-silenced U251 and U87MG cell lines using RT-qPCR to verify the effectiveness of the transfected plasmid vectors. Compared with the pcDNA3.1-NC group, DANCR expression increased significantly in U251 and U87MG cells transfected with pcDNA3.1-DANCR. Meanwhile, compared with the sh-NC group, DANCR expression in U251 and U87MG cells transfected with sh-DANCR decreased significantly (Fig. 2A and B). Then, the CCK-8 assay showed that upregulated DANCR expression could promote U251 and U87MG cell proliferation, while its inhibition slowed the rate of U251 and U87MG cell proliferation (Fig. 2C and D). Flow cytometric analysis demonstrated that the increased DANCR expression in U251 and U87MG cells reduced their apoptotic levels, while decreased DANCR expression exerted the opposite effect (Fig. 2E). Furthermore, the WB assay showed that the ATG7, beclin-1 and LC3 II/I protein levels increased and p62 levels decreased in DANCR-overexpressing U251 and U87MG cells. However, decreasing DANCR expression in U251 and U87MG cells decreased the ATG7, beclin-1 and LC3 II/I protein expression and increased p62 expression (Fig. 2F). Electron microscopic observation showed that the number of autophagosomes increased in DANCR-overexpressing U251 and U87MG cells compared with that in the control group. On the contrary, DANCR inhibition significantly reduced the number of autophagosomes in U251 and U87MG cells (Fig. 2G). In conclusion, DANCR can enhance glioma cell proliferation and autophagy and inhibit their apoptosis.

MiR-33b directly targets DANCR, regulating glioma cell autophagy, proliferation and apoptosis. To explore how DANCR functions in glioma cells, a bioinformatics database was used (starbase.sysu.edu.cn). MiR-33b was a predicted target miRNA of DANCR (Fig. 3C). Then, the targeted binding and binding site of DANCR with miR-33b were verified through a dual-luciferase reporter assay. The relative luciferase intensity of cells in the experimental group transfected with DANCR-wt + pre-miR-33b was significantly lower than that in other groups (Fig. 3D). In the present

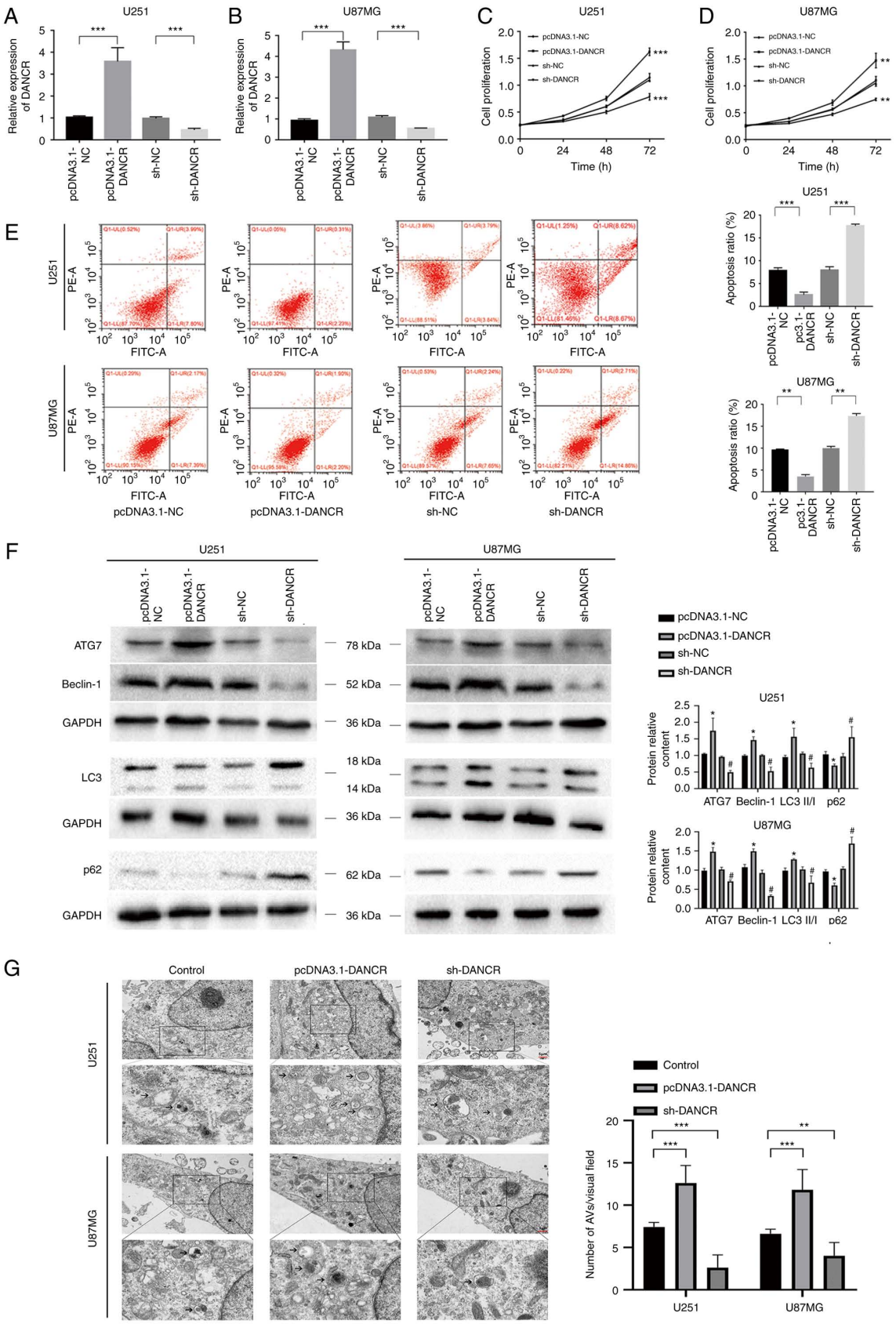

Figure 2. DANCR function in U251 and U87MG cells. (A and B) Validation of pcDNA3.1-DANCR and sh-DANCR transfection in U251 and U87MG cells (n=3). (C and D) The effects of pcDNA3.1-DANCR and sh-DANCR on U251 and U87MG cell proliferation were verified using a Cell Counting Kit-8 assay (n=3). (E) Flow cytometric analysis was used to verify the effect of pcDNA3.1-DANCR and sh-DANCR on apoptosis in U251 and U87MG cells (n=3). (F) Western blotting was used to analyze the effects of pcDNA3.1-DANCR and sh-DANCR on the ATG7, beclin-1, LC3 II/I and p62 protein expression in U251 and U87MG cells (n=3). *P<0.05 vs. pcDNA3.1-NC and $^{\#}$P<0.05 vs. sh-NC. (G) Transmission electron microscopy was used to observe the ultrastructural features of U251 and U87MG cells with altered DANCR expression. The arrow points to the autophagic vacuoles. The scale bars represent 5 μm (n=5). Data are presented as the mean ± SD. *P<0.05, **P<0.01 and ***P<0.001. DANCR, differentiation antagonizing non-protein coding RNA; sh-, short hairpin; NC, negative control; ATG7, autophagy-related 7.

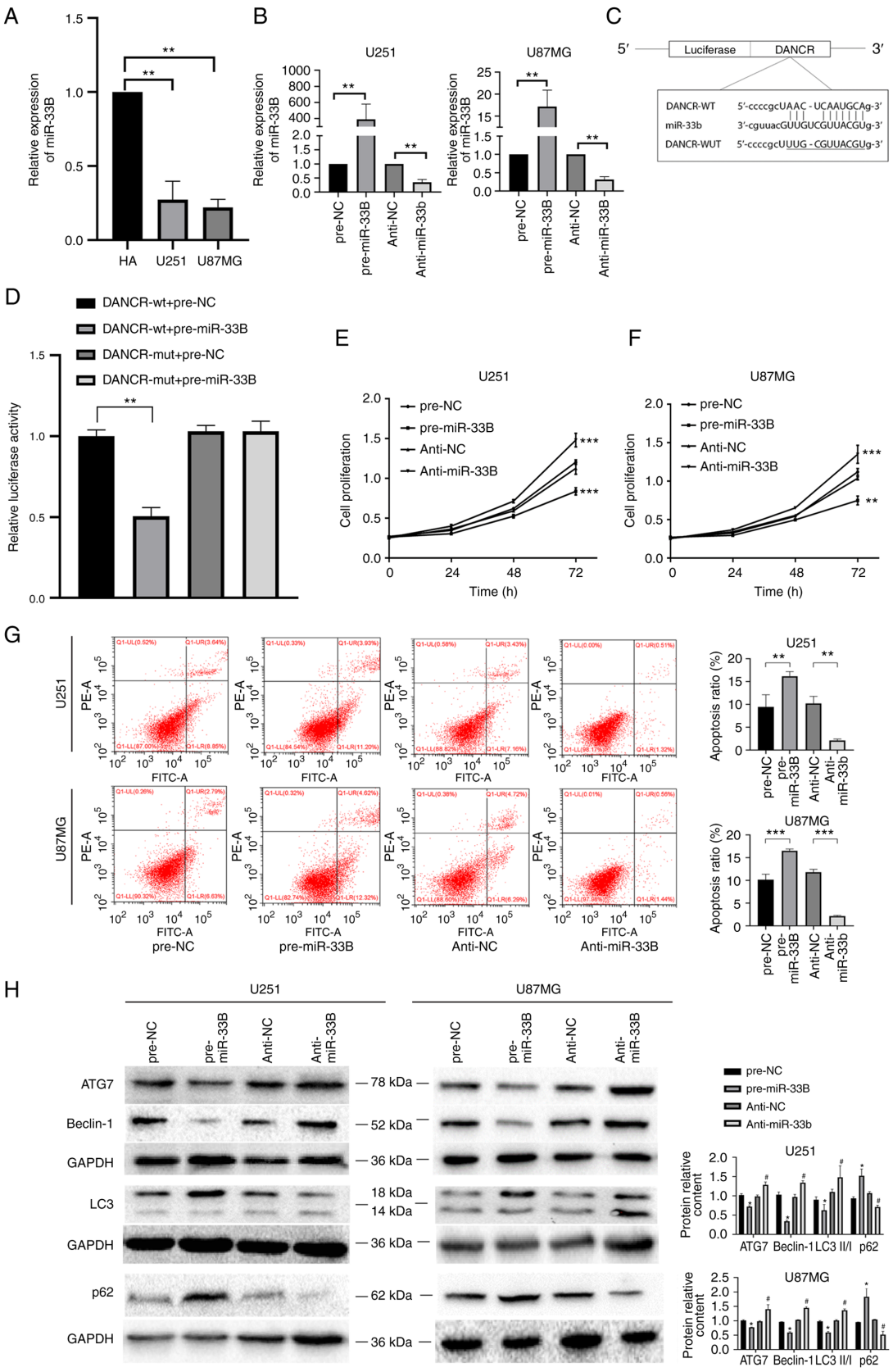

Figure 3. MiR-33b function in U251 and U87MG cells; miR-33b as a target gene of DANCR. (A) The relative miR-33b expression in HA, U251 and U87MG cells was verified using RT-qPCR (n=3). (B) Validation of pre-miR-33b and anti-miR-33b transfection in U251 and U87MG cells (n=3). (C and D) Presentation of the putative binding site of DANCR and miR-33b and relative luciferase activities of cells co-transfected with pre-miR-33b and DANCR-wt or DANCR-mut (n=3). (E and F) The effects of pre-miR-33b and anti-miR-33b on U251 and U87MG cell proliferation were verified using a Cell Counting Kit-8 assay (n=3); *P<0.05 vs. pre-NC and $^{\#}$P<0.05 vs. anti-miR-33b. (G) Flow cytometric analysis was used to verify the effects of pre-miR-33b and anti-miR-33b on apoptosis in U251 and U87MG cells (n=3). (H) Western blotting was used to analyze the effects of pre-miR-33b and anti-miR-33b on the ATG7, beclin-1, LC3 II/I and p62 protein expression in U251 and U87MG cells (n=3); *P<0.05 vs. pcDNA3.1-NC and $^{\#}$P<0.05 vs. sh-NC. Data are presented as the mean ± SD. *P<0.05, **P<0.01 and ***P<0.001. DANCR, differentiation antagonizing non-protein coding RNA; miR, microRNA; NC, negative control; HA, human astrocytes; ATG7, autophagy-related 7; wt, wild-type; mut, mutant.

study, as revealed in Fig. 3A, miR-33b expression in U251 and U87MG cells was downregulated, compared with that in HA cells. MiR-33b expression levels were then detected in miR-33b-overexpressing or miR-33b-silenced U251 and U87MG cell lines using RT-qPCR to verify the effectiveness of the transfected plasmid vectors. Compared with the pre-NC group, miR-33b expression increased significantly in U251 and U87MG cells transfected with pre-miR-33b. Meanwhile, compared with the anti-NC group, miR-33b expression in U251 and U87MG cells transfected with anti-miR-33b decreased significantly (Fig. 3B). Intracellular miR-33b expression levels were upregulated in U251 and U87MG cells and it was found that the cell proliferation slowed down (Fig. 3E and F), intracellular autophagy levels decreased, apoptotic levels increased (Fig. 3G and H), and miR-33b expression was inhibited, showing opposite effects. Hence, miR-33b may be a regulator of cell proliferation and autophagy.

miR-33b mediates the effects of DANCR on glioma cells and its function. It was explored whether miR-33b regulates the function of DANCR in glioma cells. Through co-transfection of the desired plasmid (pcDNA3.1-DANCR + pre-NC, pcDNA3.1-DANCR + pre-miR-33b, sh-DANCR + anti-NC, or sh-DANCR + anti-miR-33b) in U87MG and U251 cells, CCK-8, flow cytometry, and WB assays demonstrated that pre-miR-33b and anti-miR-33b could respectively inhibit the accelerated proliferation and decreased apoptosis or decreased proliferation and increased apoptosis caused by pcDNA3.1-DANCR or sh-DANCR. Furthermore, they respectively enhanced or slowed proliferation (Fig. 4A and B) and increased or decreased autophagy (Fig. 4C and D). These findings suggested that miR-33b is involved in regulating DANCR in glioma cells.

DLX6 knockdown restrains cell proliferation and autophagy while promoting apoptosis. Next, to research the function of DLX6 in glioma cells, WB was used to verify its protein expression level in U251, U87MG and HA cells. DLX6 expression level in the glioma cell lines U251 and U87MG was significantly higher than that in HA cells (Fig. 5A). Then, a stable sh-DLX6-transfected cell line was established and its effectiveness was verified (Fig. 5E). CCK-8 and flow cytometry showed that cell proliferation slowed down and apoptosis increased (Fig. 5B-D). Meanwhile, the WB assay verified that inhibiting DLX6 expression also decreased cell autophagy levels (Fig. 5E). These results suggested that *DLX6* knockdown slows down the progression of glioma cell malignancy.

DLX6 directly targets miR-33b and restores miR-33b-induced proliferation and autophagy reduction while reducing apoptosis. Firstly, by altering the DANCR or miR-33b levels in U251 and U87MG cells, it was found that DANCR upregulation or miR-33b downregulation increased the expression level of DLX6, while DANCR downregulation or miR-33b upregulation decreased the expression level of DLX6 (Fig. 6A and B). Then, through co-transfection of the desired plasmid (pcDNA3.1-DANCR + pre-NC, pcDNA3.1-DANCR + pre-miR-33b, sh-DANCR + anti-NC, or sh-DANCR + anti-miR-33b) in U87MG and U251 cells, it was revealed that the increased expression of DLX6 induced by DANCR was reversed by pre-miR-33b, and the decreased expression of dlx6 induced by DANCR was also reversed by anti-miR-33b (Fig. 6C). To examine the relationship between DLX6 and miR-33b, a dual-luciferase reporter assay was first employed to verify the targeted binding effect between them. The relative luciferase intensity of cells in the experimental group transfected with DLX6-WT and pre-miR-33b was significantly lower than that in other groups (Fig. 6D and E). Then, U87 and U251 glioma cells were co-transfected with anti-miR-33b + sh-DLX6, and cells co-transfected with anti-miR-33b + sh-NC were set as a negative control. CCK-8 and flow cytometric assays showed that *DLX6* knockdown could reverse the increase in the degree of malignant glioma cells caused by the decreased miR-33b expression (Fig. 6F-H). In addition, WB also verified that *DLX6* knockdown reversed the increase in autophagy caused by decreased miR-33b expression (Fig. 6I). The aforementioned results demonstrated that DLX6 is involved in the regulation of miR-33b in the progression of glioma cell malignancy.

ATG7 is involved in DLX6-mediated autophagy in glioma cells. Jaspar predicted DLX6 as an ATG7 transcription factor, the predicted binding site was located between 2,000 base pairs (bp) upstream and 1,000 bp downstream of the transcription start site (TSS), and the control sequence was between 2,000 and 3,000 bp upstream of the TSS (Fig. 7A). A ChIP assay was used to verify whether DLX6 directly binds to the promoter sequence of ATG7 and regulates its transcription, and the same conclusion was obtained (Fig. 7B). Meanwhile, a WB assay verified that ATG7 expression level could be inhibited by *DLX6* knockdown in U251 and U87MG cells (Fig. 5E). Thus, DLX6 is a transcription factor of ATG7 and promotes its expression.

DANCR and DLX6 knockdown combined with miR-33b overexpression inhibit ectopic tumor growth and ATG7 expression in mice. To further confirm the aforementioned conclusion, *in vivo* experiments were conducted. The results showed that the tumor volumes in the sh-DANCR, pre-miR-33b, sh-DLX6 and sh-DANCR + pre-miR-33b + sh-DLX6 groups were smaller than that in the control group. The tumor volume was smallest in the group with *DANCR* and *DLX6* knockdown combined with miR-33b overexpression (Fig. 8A-C). When ATG7 protein levels were measured *in vitro* via immunohistochemistry, it was found that they were lower in the sh-DANCR, pre-miR-33b, sh-DLX6 and sh-DANCR + pre-miR-33b + sh-DLX6 groups than in the control group, and ATG7 protein levels were the lowest in the sh-DANCR + pre-miR-33b + sh-DLX6 group (Fig. 8D).

Discussion

In the present study, it was found that DANCR expression is upregulated in glioma cells. By regulating DANCR expression in glioma cells, it was revealed that proliferation and autophagy levels in glioma cells were positively associated with DANCR expression, while the apoptosis ratio showed an inverse association. By contrast, miR-33b plays a tumor suppressor role in gliomas. MiR-33b could bind with the 3'-UTR of DLX6 and inhibit its function. DLX6 is a transcription factor of

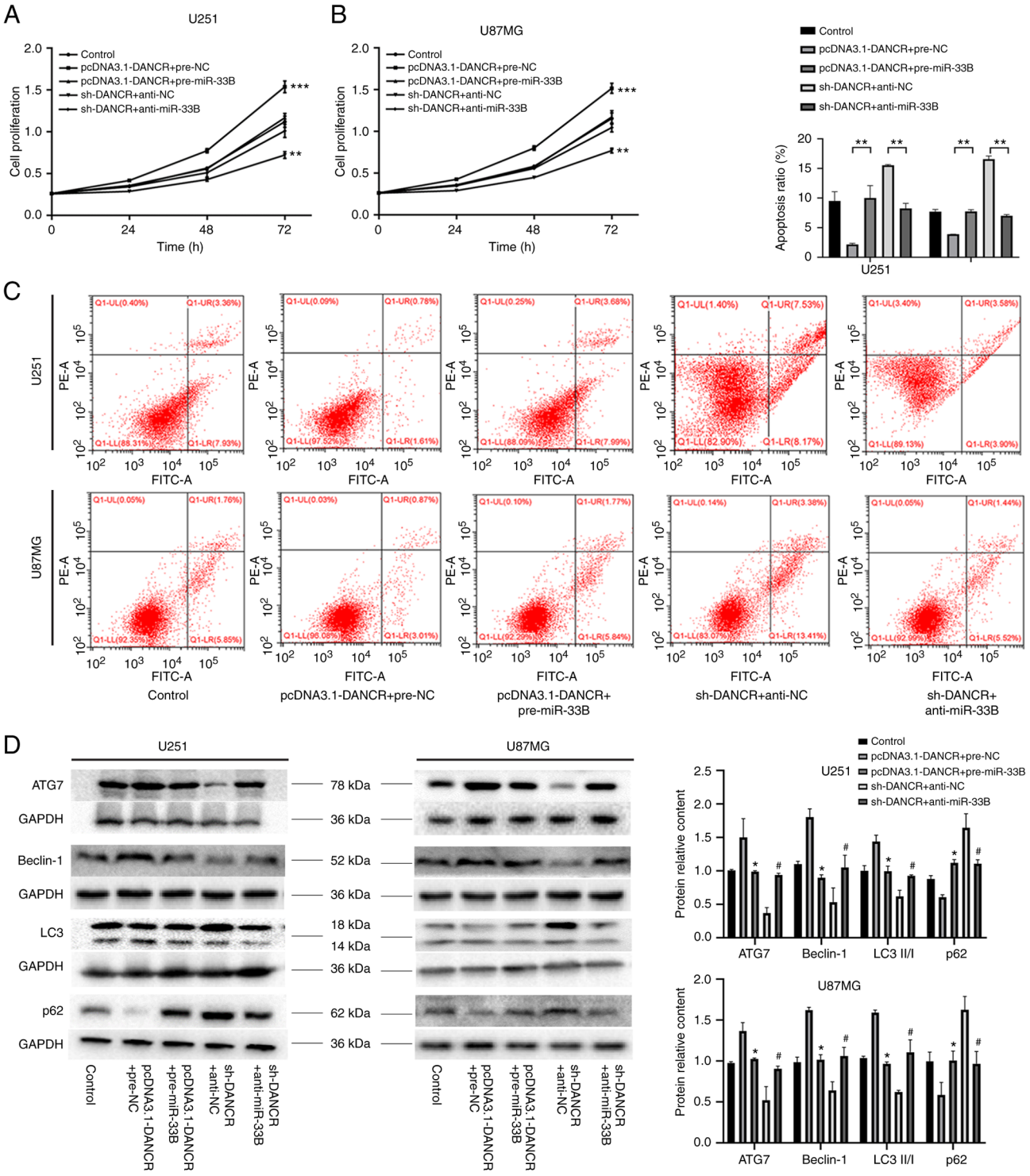

Figure 4. MiR-33b exerts opposite effects to DANCR and can reverse the changes caused by *DANCR* overexpression or knockdown. (A and B) Cell Counting Kit-8 assay was used to detect the change in proliferation due to DANCR overexpression via transfection of pre-NC or pre-miR-33b, as well as the effects of anti-NC and anti-miR-33b on *DANCR*-knockdown cells (n=3). (C) Flow cytometric analysis was conducted to determine the apoptosis ratio of U251 and U87MG cells co-transfected with DANCR and miR-33b (n=3). (D) Changes in autophagy levels in U251 and U87MG cells co-transfected with DANCR and miR-33b were verified via western blotting of the autophagy-related proteins ATG7, beclin-1, LC3 II/I, and p62 (n=3); *P<0.05 vs. pcDNA3.1-DANCR + pre-miR-NC; $^{\#}$P<0.05 vs. sh-DANCR + anti-miR-33b. Data are presented as the mean ± SD. *P<0.05, **P<0.01 and ***P<0.001. miR, microRNA; DANCR, differentiation antagonizing non-protein coding RNA; NC, negative control; ATG7, autophagy-related 7; sh-, short hairpin.

ATG7 and can promote its transcription. Therefore, DANCR indirectly promotes DLX6 expression and *ATG7* transcription by reducing the targeted connection between miR-33b and DLX6 3'-UTR by sponging miR-33b. Finally, *DANCR* and *DLX6* knockdown combined with simultaneous miR-33b overexpression showed the strongest inhibitory effect of tumor growth in the present study.

As a common non-coding RNA, lncRNA involvement has been demonstrated in the progression of various tumors (25). DANCR, as an lncRNA, has also been reported to promote

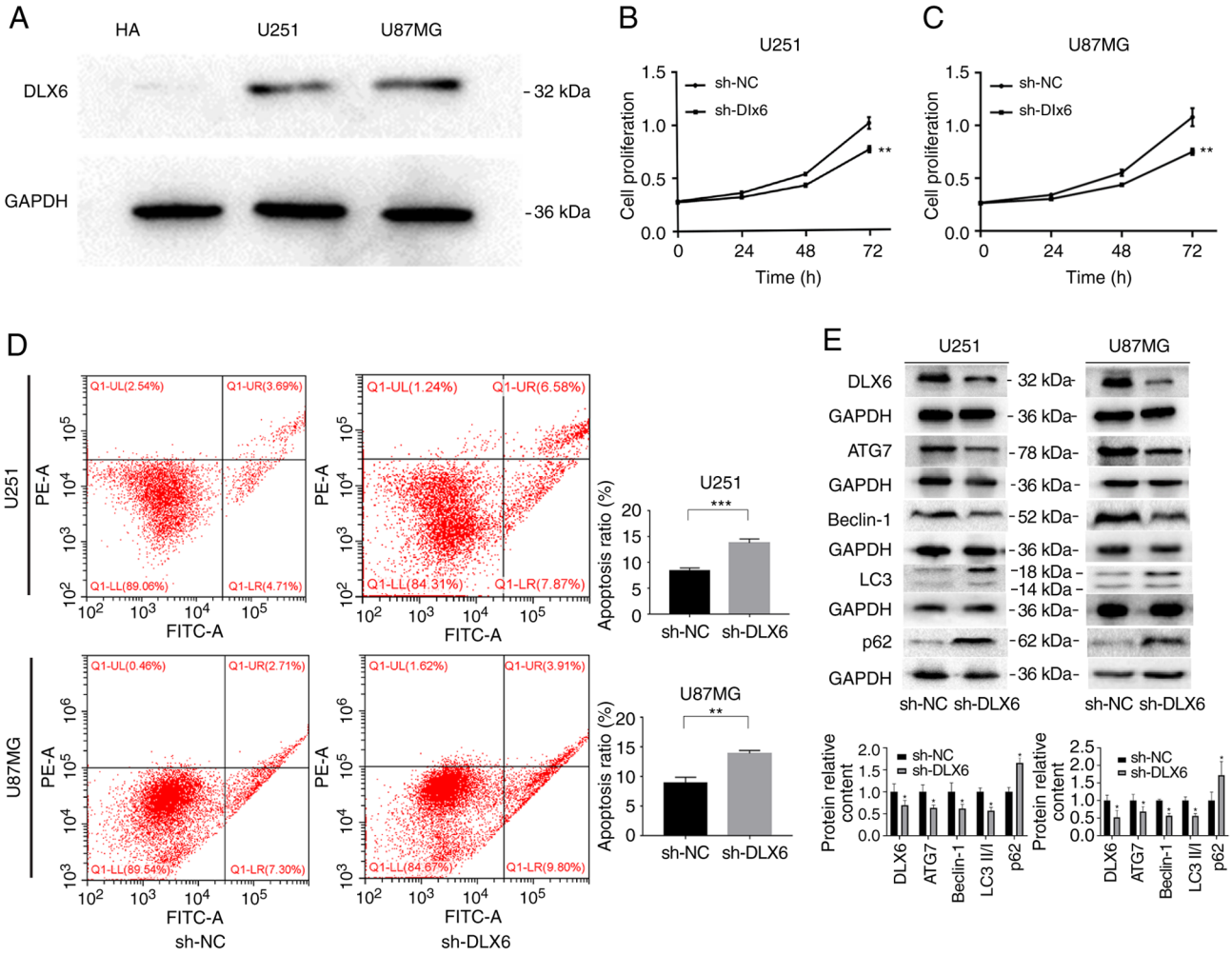

Figure 5. DLX6 function in U251 and U87MG cells. (A) DLX6 expression verified via western blotting was upregulated in U251 and U87MG cells, compared with that in HA cells (n=3). (B-D) Cell Counting Kit-8 and flow cytometric assays were used to verify the effect of *DLX6* knockdown on proliferation and apoptosis in U251 and U87MG cells (n=3). (E) The effectiveness of sh-DLX6 was verified, and the ATG7, beclin-1, LC3 II/I, and p62 protein expression in each group was detected via western blot assays (n=3). Data are presented as the mean ± SD. *P<0.05 vs. sh-NC. *P<0.05, **P<0.01 and ***P<0.001. DLX6, distal-less homeobox 6; HA, human astrocytes; ATG7, autophagy-related 7; NC, negative control; sh-, short hairpin.

the progression of various malignant tumors (5). In the present study, DANCR was upregulated in glioma cells and promoted malignant glioma progression by promoting proliferation and autophagy and inhibiting apoptosis. Previous studies have reported that DANCR is highly expressed in glioma tissues and cells and plays a function in the progression of glioma malignancy and cisplatin resistance (26,27). DANCR regulates colon cancer cell desensitization to cisplatin by sponging miR-125B-5p as a competing endogenous RNA (ceRNA), and sponging miR-335 regulates the lymphatic metastasis of bladder cancer (28,29). By inhibiting DANCR expression, the progression of glioma cell malignancy can be inhibited, and its effect is exerted through miR-135a sponging (30). DANCR enhances cytarabine resistance in acute myeloid leukemia by promoting autophagy through miR-874-3p sponging (31). The aforementioned conclusions were also verified by the present experimental results. DANCR can increase the level of autophagy and progression of glioma cell malignancy and interact with miRNA as a ceRNA.

There is increasing evidence that miRNAs play an important role in the progression of cancer malignancy. MiRNA can act as a tumor suppressor in lung, prostate and breast cancers (32-34). Evidence also shows that miR-93 plays a role in inhibiting autophagy in glioma (10). Other researchers have shown that miR-33b plays a role in prostate cancer and renal cell carcinoma, where it also acts as a prognostic factor; in addition, low miR-33b expression can promote peritoneal metastasis of ovarian cancer cells and aggravate cancer progression (13,14,35). In the present study, miR-33b was highly expressed in glioma cells, which was also observed in the results of Qi and Gao (36). MiR-33b overexpression can inhibit proliferation and autophagy and promote apoptosis in glioma cells. Furthermore, it can inhibit enhanced proliferation and autophagy and reduce apoptosis in glioma cells caused by DANCR overexpression. On the contrary, miR-33b inhibition can reverse the decreased proliferation, autophagy and apoptosis in glioma cells caused by DANCR inhibition. The present study revealed miR-33b as a possible ceRNA of DANCR, which regulated its function.

In the present study, it was identified that miR-33b can bind to the 3'-UTR of DLX6 and regulate its expression. Liang *et al* (18) showed that DLX6 can promote oral

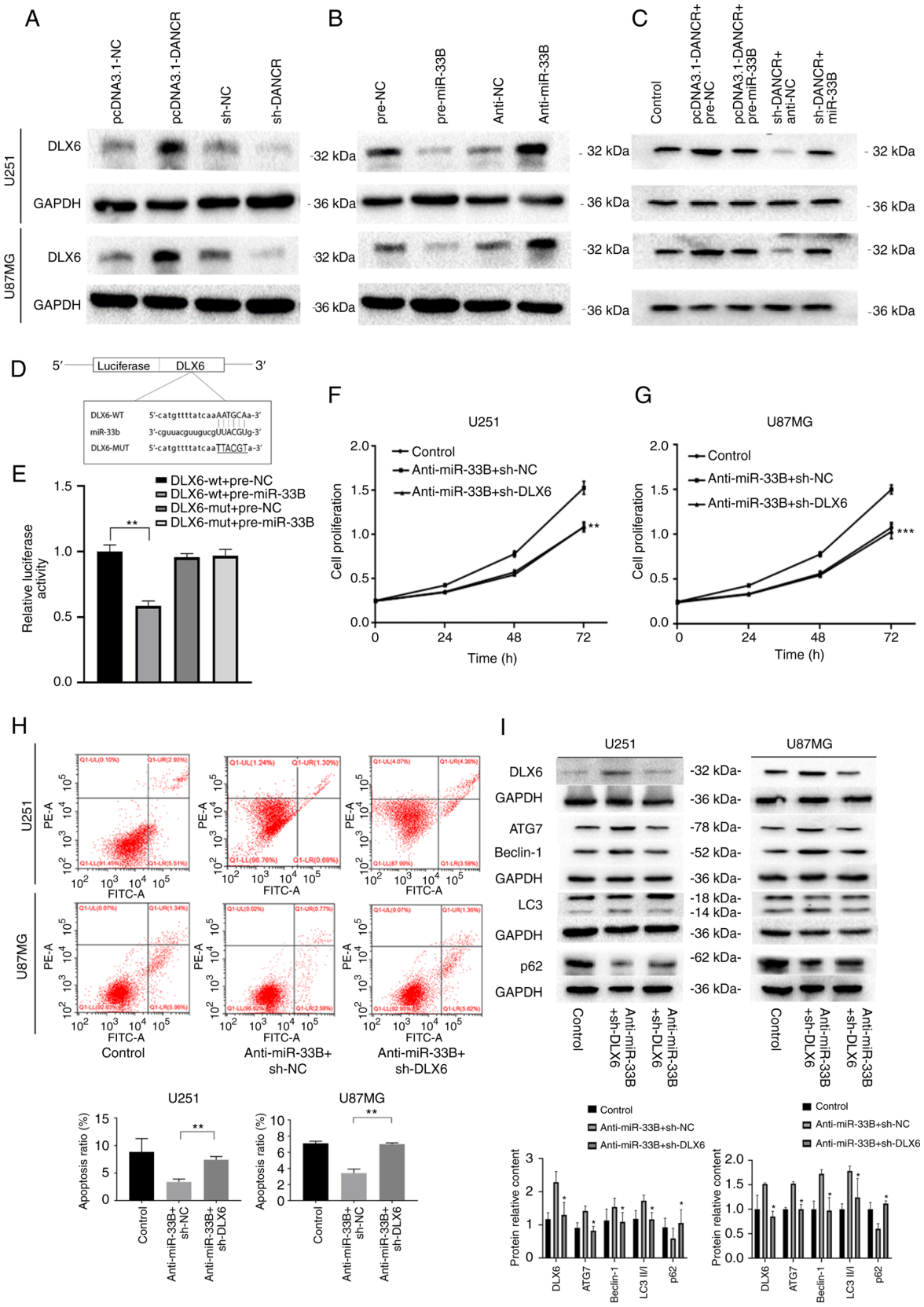

Figure 6. The effects of DLX6 on DLX6 and sh-DLX6 expression could reverse the effects of anti-miR-33b on U251 and U87MG cell proliferation, autophagy and apoptosis. (A-C) The effects of DANCR and miR-33b alone and in combination on DLX6 protein expression in U251 and U87MG cells were verified via western blotting (n=3). (D) Presentation of the putative binding site of DLX6 and miR-33b. (E) Relative luciferase activities of cells co-transfected with pre-miR-33b and DLX6-wt or DLX6-mut (n=3). (F and G) Cell Counting Kit-8 assay was used to detect the change in proliferation of *DLX6*-knockdown U251 and U87MG cells transfected with anti-NC or anti-miR-33b (n=3). (H) Flow cytometric analysis was conducted to determine the apoptosis ratio of U251 and U87MG cells co-transfected with sh-DLX6 and anti-miR-33b (n=3). (I) The protein expression of ATG7, beclin-1, LC3 II/I and p62 in each group were detected using western blot assays (n=3). *P<0.05 vs. anti-miR-33b + sh-NC. Data are presented as mean ± SD. *P<0.05, **P<0.01 and ***P<0.001. DLX6, distal-less homeobox 6; sh-, short hairpin; DANCR, differentiation antagonizing non-protein coding RNA; miR, microRNA; wt, wild-type; mut, mutant; NC, negative control; ATG7, autophagy-related 7.

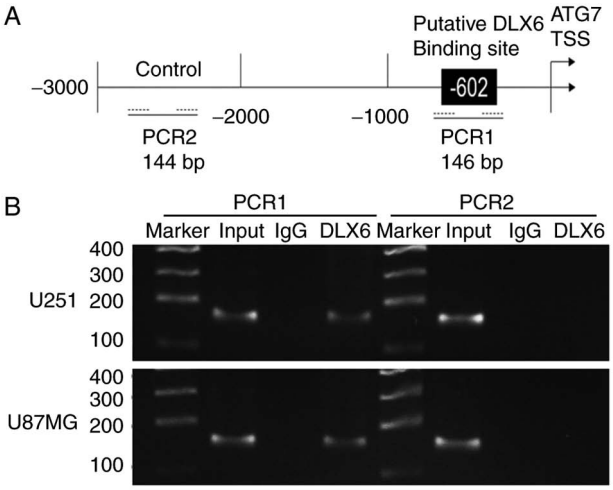

Figure 7. Chromatin immunoprecipitation assay demonstrated that DLX6 directly binds to the *ATG7* promoter in U251 and U87MG cells. (A) The putative DLX6 binding site located at the DLX6 promoter region 602 bp upstream of the TSS. (B) Immunoprecipitated DNA was amplified via PCR. Normal rabbit IgG was used as a negative control. DLX6, distal-less homeobox 6; TSS, transcription start site.

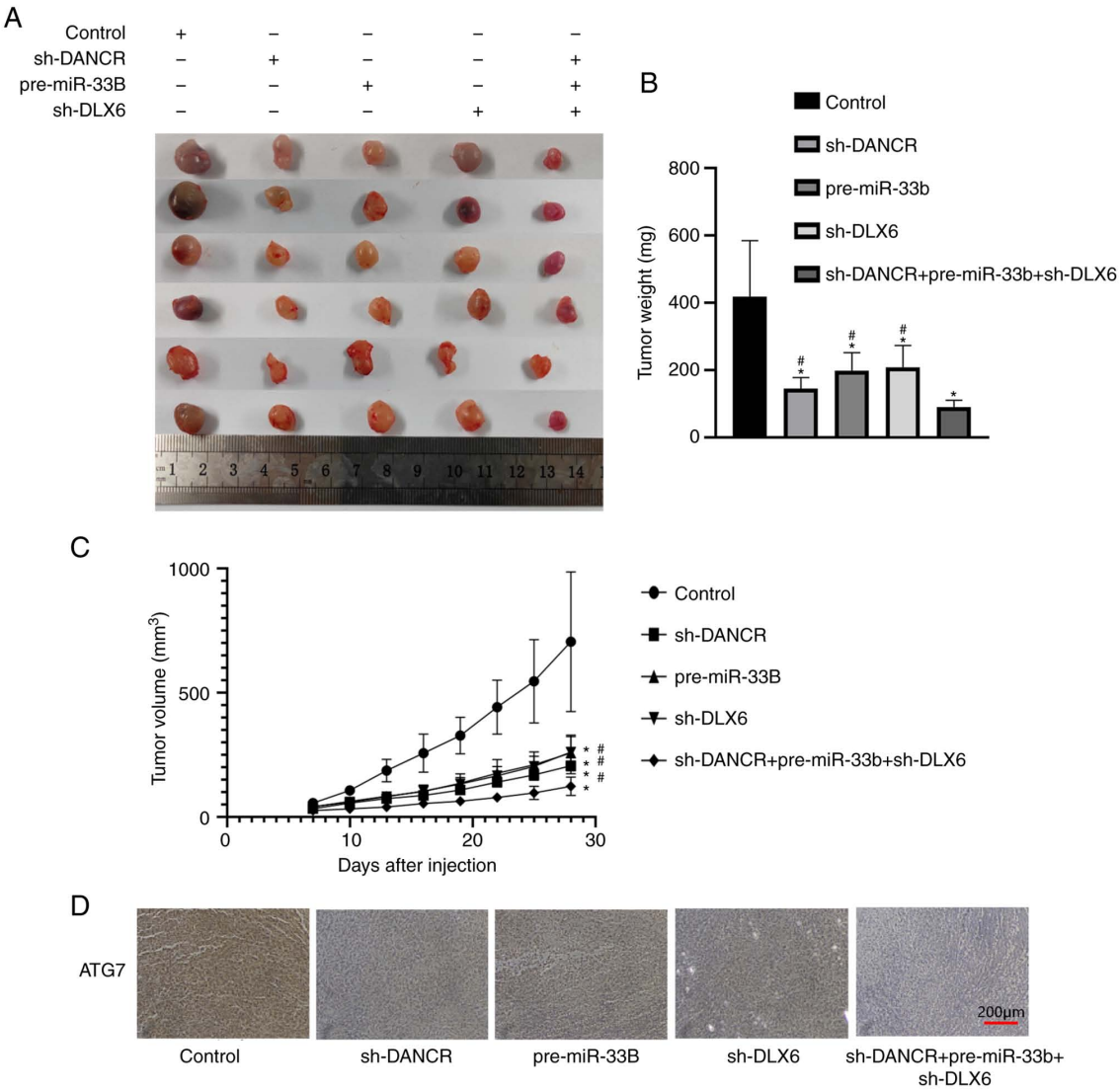

Figure 8. *In vivo* study. (A) *In vivo* and *in vitro* samples from different groups of tumors. (B) Tumor weight in each group. *P<0.05 vs. control; #P<0.05 vs. sh-DANCR + pre-miR-33b + sh-DLX6. Data are presented as the mean ± SD (n=6 in each group). (C) Tumor volume change curves for each group. *P<0.05 vs. control; #P<0.05 vs. sh-DANCR + pre-miR-33b + sh-DLX6. Data are presented as the mean ± SD (n=6 in each group). (D) Immunohistochemical analysis of ATG7 in tumors from each group. The scale bars represent 200 μm. DANCR, differentiation antagonizing non-protein coding RNA; sh-, short hairpin; miR, microRNA; DLX6, distal-less homeobox 6.

squamous cell carcinoma cell proliferation and survival. However, the relationship between DLX6 and glioma has not been reported. The present study found that DLX6 expression was upregulated in glioma, and inhibiting it could inhibit the proliferation and autophagy of glioma cells and promote apoptosis. Moreover, inhibition of DLX6 could reverse the inhibition of miR-33b-induced proliferation and autophagy enhancement and apoptosis reduction in glioma. DLX6 was revealed to be a transcription factor of *ATG7* that could directly regulate its expression. However, whether DLX6 is involved in the transcription of other autophagy-related transgenes needs further investigation. In autophagy, ATG7 plays an important role in processes, such as the transformation of LC3 I to LC3 II and the transport of autophagic vesicles in the cytoplasm (37). In addition, Atg12-Atg5 and LC3-lipid/membrane ubiquitin-like conjugation systems are the core machinery for autophagosome formation (38). Lung cancer studies have shown that ATG7 expression promotes the progression of lung cancer malignancy by promoting autophagy and drug resistance in lung cancer cells (39-41). However, the drug resistance of glioma was not studied in this study, so whether DANCR can affect drug resistance by regulating ATG7-induced autophagy needs to be further studied. A recent study in mice showed that ATG7-related autophagy promoted anti-tumor immunity, thereby promoting tumor-cell survival (42). Hypoxia in glioma cells can induce intracellular protective autophagy, thus affecting glioma progression (43). Glioma cells can meet the intracellular capacity demand through autophagy-mediated lipid metabolism, thereby promoting their malignancy (44). The aforementioned studies indirectly support the findings of the present study.

In summary, it was demonstrated that DANCR expression is upregulated in glioma cells and that DLX6 expression level is upregulated via inhibition of the targeted sponge interaction between miR-33b and DLX6. DLX6 activates ATG7 expression by binding to its promoter region, enhancing intracellular autophagy and affecting the progression of glioma cell malignancy. In conclusion, DANCR upregulates ATG7 protein expression through the miR-33b/DLX6 pathway, thereby enhancing intracellular autophagy and promoting progression in glioma cell malignancy, inhibiting tumor proliferation and protecting autophagy while promoting tumor cell apoptosis. In addition, it was identified that miR-33b was negatively regulated by the miRNA sponge-like role of DANCR. Mir-33b could bind to the 3'-UTR of DLX6 and suppress ATG7 expression through negative regulation of DLX6, thus inhibiting the progression of glioma cell malignancy.

Acknowledgements

Not applicable.

Funding

The present study was supported by the Liaoning Science and Technology Plan Project (grant no. 2018225094) and the Natural Science Foundation of Liaoning Province (grant no. 2020-MS-165).

Availability of data and materials

The datasets used and/or analyzed during the current study are available from the corresponding author on reasonable request.

Authors' contributions

XXL designed the experiments and preliminary validation. WY conducted the experiments. LM analyzed and processed the data. XXL, WY and LM wrote and modified the manuscript. All authors read and approved the final version of the manuscript and confirm the authenticity of all the raw data.

Ethics approval and consent to participate

The present study was approved (approval no. 2022PS021K) by the Medical Ethics Committee of Shengjing Hospital (Shenyang, China).

Patient consent for publication

Not applicable.

Competing interests

The authors declare that they have no competing interests.

References

1. Lapointe S, Perry A and Butowski NA: Primary brain tumours in adults. Lancet 392: 432-446, 2018.
2. Chen R, Smith-Cohn M, Cohen AL and Colman H: Glioma subclassifications and their clinical significance. Neurotherapeutics 14: 284-297, 2017.
3. Ostrom QT, Bauchet L, Davis FG, Deltour I, Fisher JL, Langer CE, Pekmezci M, Schwartzbaum JA, Turner MC, Walsh KM, *et al*: The epidemiology of glioma in adults: A 'state of the science' review. Neuro Oncol 16: 896-913, 2014.
4. ENCODE Project Consortium: An integrated encyclopedia of DNA elements in the human genome. Nature 489: 57-74, 2012.
5. Wang M, Gu J, Zhang X, Yang J, Zhang X and Fang X: Long non-coding RNA DANCR in cancer: Roles, mechanisms, and implications. Front Cell Dev Biol 9: 753706, 2021.
6. Hu X, Peng WX, Zhou H, Jiang J, Zhou X, Huang D, Mo YY and Yang L: IGF2BP2 regulates DANCR by serving as an N6-methyladenosine reader. Cell Death Differ 27: 1782-1794, 2020.
7. Zhen Q, Gao LN, Wang RF, Chu WW, Zhang YX, Zhao XJ, Lv BL and Liu JB: LncRNA DANCR promotes lung cancer by sequestering miR-216a. Cancer Control 25: 1073274818769849, 2018.
8. Hill M and Tran N: miRNA interplay: Mechanisms and consequences in cancer. Dis Model Mech 14: dmm047662, 2021.
9. Carthew RW and Sontheimer EJ: Origins and mechanisms of miRNAs and siRNAs. Cell 136: 642-655, 2009.
10. Huang T, Wan X, Alvarez AA, James CD, Song X, Yang Y, Sastry N, Nakano I, Sulman EP, Hu B and Cheng SY: MIR93 (microRNA-93) regulates tumorigenicity and therapy response of glioblastoma by targeting autophagy. Autophagy 15: 1100-1111, 2019.
11. Cao HL, Liu ZJ, Huang PL, Yue YL and Xi JN: lncRNA-RMRP promotes proliferation, migration and invasion of bladder cancer via miR-206. Eur Rev Med Pharmacol Sci 23: 1012-1021, 2019.
12. Hessam S, Sand M, Skrygan M, Gambichler T and Bechara FG: Expression of miRNA-155, miRNA-223, miRNA-31, miRNA-21, miRNA-125b, and miRNA-146a in the inflammatory pathway of hidradenitis suppurativa. Inflammation 40: 464-672, 2017.
13. Huang G, Lai Y, Pan X, Zhou L, Quan J, Zhao L, Li Z, Lin C, Wang J, Li H, *et al*: Tumor suppressor miR-33b-5p regulates cellular function and acts a prognostic biomarker in RCC. Am J Transl Res 12: 3346-3360, 2020.

14. Zhao M, Qi M, Li X, Hu J, Zhang J, Jiao M, Bai X, Peng X and Han B: CUL4B/miR-33b/C-MYC axis promotes prostate cancer progression. Prostate 79: 480-488, 2019.
15. Lv SQ, Kim YH, Giulio F, Shalaby T, Nobusawa S, Yang H, Zhou Z, Grotzer M and Ohgaki H: Genetic alterations in microRNAs in medulloblastomas. Brain Pathol 22: 230-239, 2012.
16. Simeone A, Acampora D, Pannese M, D'Esposito M, Stornaiuolo A, Gulisano M, Mallamaci A, Kastury K, Druck T, Huebner K, *et al*: Cloning and characterization of two members of the vertebrate Dlx gene family. Proc Natl Acad Sci USA 91: 2250-2254, 1994.
17. Batista-Brito R, Machold R, Klein C and Fishell G: Gene expression in cortical interneuron precursors is prescient of their mature function. Cereb Cortex 18: 2306-2317, 2008.
18. Liang J, Liu J, Deng Z, Liu Z and Liang L: DLX6 promotes cell proliferation and survival in oral squamous cell carcinoma. Oral Dis 28: 87-96, 2022.
19. Collier JJ, Oláhová M, McWilliams TG and Taylor RW: ATG7 safeguards human neural integrity. Autophagy 17: 2651-2653, 2021.
20. Klionsky DJ, Petroni G, Amaravadi RK, Baehrecke EH, Ballabio A, Boya P, Bravo-San Pedro JM, Cadwell K, Cecconi F, Choi AMK, *et al*: Autophagy in major human diseases. EMBO J 40: e108863, 2021.
21. White E: The role for autophagy in cancer. J Clin Invest 125: 42-46, 2015.
22. Zhu J, Tian Z, Li Y, Hua X, Zhang D, Li J, Jin H, Xu J, Chen W, Niu B, *et al*: ATG7 promotes bladder cancer invasion via autophagy-mediated increased ARHGDIB mRNA stability. Adv Sci (Weinh) 6: 1801927, 2019.
23. Li J, Tang C, Li L, Li R and Fan Y: Quercetin blocks t-AUCB-induced autophagy by Hsp27 and Atg7 inhibition in glioblastoma cells in vitro. J Neurooncol 129: 39-45, 2016.
24. Livak KJ and Schmittgen TD: Analysis of relative gene expression data using real-time quantitative PCR and the 2(-Delta Delta C(T)) method. Methods 25: 402-408, 2001.
25. Peng WX, Koirala P and Mo YY: LncRNA-mediated regulation of cell signaling in cancer. Oncogene 36: 5661-5667, 2017.
26. Ma Y, Zhou G, Li M, Hu D, Zhang L, Liu P and Lin K: Long noncoding RNA DANCR mediates cisplatin resistance in glioma cells via activating AXL/PI3K/Akt/NF-κB signaling pathway. Neurochem Int 118: 233-241, 2018.
27. Li J and Zhou L: Overexpression of lncRNA DANCR positively affects progression of glioma via activating Wnt/β-catenin signaling. Biomed Pharmacother 102: 602-607, 2018.
28. Ping Q, Shi Y, Yang M, Li H, Zhong Y, Li J, Bi X and Wang C: LncRNA DANCR regulates lymphatic metastasis of bladder cancer via the miR-335/VEGF-C axis. Transl Androl Urol 10: 1743-1753, 2021.
29. Shi H, Li K, Feng J, Liu G, Feng Y and Zhang X: LncRNA-DANCR interferes with miR-125b-5p/HK2 axis to desensitize colon cancer cells to cisplatin vis activating anaerobic glycolysis. Front Oncol 10: 1034, 2020.
30. Feng L, Lin T, Che H and Wang X: Long noncoding RNA DANCR knockdown inhibits proliferation, migration and invasion of glioma by regulating miR-135a-5p/BMI1. Cancer Cell Int 20: 53, 2020.
31. Zhang H, Liu L, Chen L, Liu H, Ren S and Tao Y: Long noncoding RNA DANCR confers cytarabine resistance in acute myeloid leukemia by activating autophagy via the miR-874-3P/ATG16L1 axis. Mol Oncol 15: 1203-1216, 2021.
32. Sur S, Steele R, Shi X and Ray RB: miRNA-29b inhibits prostate tumor growth and induces apoptosis by increasing bim expression. Cells 8: 1455, 2019.
33. Su WZ and Ren LF: MiRNA-199 inhibits malignant progression of lung cancer through mediating RGS17. Eur Rev Med Pharmacol Sci 23: 3390-3400, 2019.
34. Kong X, Duan Y, Sang Y, Li Y, Zhang H, Liang Y, Liu Y, Zhang N and Yang Q: LncRNA-CDC6 promotes breast cancer progression and function as ceRNA to target CDC6 by sponging microRNA-215. J Cell Physiol 234: 9105-9117, 2019.
35. Wang X, Yung MMH, Sharma R, Chen F, Poon YT, Lam WY, Li B, Ngan HYS, Chan KKL and Chan DW: Epigenetic silencing of miR-33b promotes peritoneal metastases of ovarian cancer by modulating the TAK1/FASN/CPT1A/NF-κB axis. Cancers (Basel) 13: 4795, 2021.
36. Qi Y and Gao Y: Clinical significance of miR-33b in glioma and its regulatory role in tumor cell proliferation, invasion and migration. Biomark Med 14: 539-548, 2020.
37. Nishida Y, Arakawa S, Fujitani K, Yamaguchi H, Mizuta T, Kanaseki T, Komatsu M, Otsu K, Tsujimoto Y and Shimizu S: Discovery of Atg5/Atg7-independent alternative macroautophagy. Nature 461: 654-658, 2009.
38. Xie Z and Klionsky DJ: Autophagosome formation: Core machinery and adaptations. Nat Cell Biol 9: 1102-1109, 2007.
39. Pan X, Chen Y, Shen Y and Tantai J: Knockdown of TRIM65 inhibits autophagy and cisplatin resistance in A549/DDP cells by regulating miR-138-5p/ATG7. Cell Death Dis 10: 429, 2019.
40. Wang H, Guo M, Ding D, Yang F and Chen Z: Long non-coding RNA NNT-AS1 contributes to cisplatin resistance via miR-1236-3p/ATG7 axis in lung cancer cells. Onco Targets Ther 13: 3641-3652, 2020.
41. Pan R and Zhou H: Exosomal transfer of lncRNA H19 promotes erlotinib resistance in non-small cell lung cancer via miR-615-3p/ATG7 axis. Cancer Manag Res 12: 4283-4297, 2020.
42. Arensman MD, Yang XS, Zhong W, Bisulco S, Upeslacis E, Rosfjord EC, Deng S, Abraham RT and Eng CH: Anti-tumor immunity influences cancer cell reliance upon ATG7. Oncoimmunology 9: 1800162, 2020.
43. Feng X, Zhang H, Meng L, Song H, Zhou Q, Qu C, Zhao P, Li Q, Zou C, Liu X and Zhang Z: Hypoxia-induced acetylation of PAK1 enhances autophagy and promotes brain tumorigenesis via phosphorylating ATG5. Autophagy 17: 723-742, 2021.
44. Wang C, Haas MA, Yeo SK, Paul R, Yang F, Vallabhapurapu S, Qi X, Plas DR and Guan JL: Autophagy mediated lipid catabolism facilitates glioma progression to overcome bioenergetic crisis. Br J Cancer 124: 1711-1723, 2021.